Spectrochimica Acta Part B 147 (2018) 28–42

Contents lists available at ScienceDirect

Spectrochimica Acta Part B

journal homepage: www.elsevier.com/locate/sab

Towards routine analysis of TiO_2 (nano-)particle size in consumer products: Evaluation of potential techniques

Inmaculada de la Calle[a,b,*], Mathieu Menta[a], Marlène Klein[a], Benoît Maxit[c], Fabienne Séby[a]

[a] Ultra Trace Analyses Aquitaine UT2A/ADERA, Hélioparc Pau-Pyrénées, 2 avenue du Président Angot, 64053 PAU cedex 9, Pau, France
[b] Departamento de Química Analítica y Alimentaria, Área de Química Analítica, Facultad de Química, Universidad de Vigo, Campus As Lagoas-Marcosende s/n, 36310 Vigo, Spain
[c] Cordouan Technologies, Cité de la Photonique, 11 Avenue Canteranne, 33600 Pessac, France

ARTICLE INFO

Keywords:
TiO_2 nanoparticles
DLS
spICP-MS
AF4-MALS-(sp)ICP-MS
Microscopy

ABSTRACT

In this work, the potential of several techniques commonly used in research studies for TiO_2 nanoparticles' (NPs) characterization was evaluated for the implementation in routine analysis. Namely, Dynamic Light Scattering (DLS), single-particle mode Inductively Coupled Plasma Mass Spectrometry (spICP-MS) and Asymmetrical Flow Field-Flow Fractionation coupled to Multi Angle Light Scattering and (single particle) Inductively-Coupled Plasma Mass Spectrometry (AF4-MALS-(sp)ICP-MS) were assessed for this purpose. Electron Microscopy was also used to confirm the validity of results and to obtain information about the shape of the particles. Each instrument was optimized according to routine analysis criteria using reference materials for instrument performance and quality assurance. Then, the methodology was applied to two types of samples of consumer products (sunscreens and sugar-coated chocolate candies), where particle size and concentration obtained by each technique were discussed. Results indicated that TiO_2 particles were found in both samples. AF4-MALS-ICP-MS and spICP-MS were powerful tools to characterize TiO_2 NPs in real samples, with spICP-MS being more adapted to routine analysis. DLS and electron microscopy provided comparable results for the particle size. The studied sunscreen complied with the European regulation (No 1223/2009) in relation with NPs because the particle size found for TiO_2 was in the range 80–110 nm and the reference to "nano" required is present in the label of the product. Sugar-coated chocolate candies may contain NPs according to DLS and AF4-MALS-ICP-MS results, but particles larger than 100 nm were found by spICP-MS.

1. Introduction

In the last few years, the use of nanoparticles (NPs) has increased in different daily products, such as cosmetics or food. Due to their possible toxicological effects on the human body and other living organisms, as well as their potential impact on the environment, legislation has started to be implemented at a European level. Indeed, the European Commission (EC) has already recommended the definition of a nanomaterial (NMs) as a material with 50% or more of the particles in number-based size distribution in the range 1–100 nm [1].

According to the regulations EC No 1223/2009 [2] and No 1169/2011 [3], the presence of NPs in consumer products requires the addition of the word "nano" between brackets in the list of ingredients in cosmetics and food products, respectively. For cosmetics, only TiO_2 and ZnO in nanoform are allowed as inorganic ultraviolet (UV) filters to protect the skin against UV radiation but their presence needs to be mentioned in the label [2,4]. Concerning food products, the current European regulation still remains unclear, particularly for food additives containing NPs. The presence of calcium carbonate (E170), vegetable carbon (E170) and titanium dioxide (E171) is allowed in nanoforms, but the particle size should be included in the specifications of the product [3]. In the case of TiO_2, the European Food Safety Authority (EFSA) recently concluded that its use as a food additive does not raise genotoxic effects and more reliable data are still needed to show its impact on the reproductive functions [5]. Other additives such as iron oxides and hydroxides (E172), silver (E174) and gold (E175), silicon dioxide (E551), calcium silicate (E552), magnesium silicate (E553a) and talc (hydrated magnesium silicate) (E553b) will be evaluated in the next few years. In relation to the properties describing NPs, the EC only focuses on the size (mean diameter) and number-based size distribution. Other properties necessary for evaluation in the future for consumer products will be particle shape, chemical composition, charge, surface area, stability, etc. These parameters can be related to their behavior, interaction with biological systems, fate, effects and

* Corresponding author at: Ultra Trace Analyses Aquitaine UT2A/ADERA, Hélioparc Pau-Pyrénées, 2 avenue du Président Angot, 64053 PAU cedex 9, Pau, France.
E-mail address: incalle@uvigo.es (I. de la Calle).

https://doi.org/10.1016/j.sab.2018.05.012
Received 23 November 2017; Received in revised form 12 May 2018; Accepted 15 May 2018
Available online 19 May 2018

degradation (by oxidation reactions) [6].

Several works have been published describing sample preparation before the analysis of TiO_2 NPs in cosmetics [7–20] and foods [9,21–25]. For cosmetics, direct analysis of the sample or its dispersion in ethanol before deposition onto a support [7,14,15], resin embedding [10] or only dispersion in water/ethanol [12,14] were used. In most studies, a degreasing step is applied using organic solvent (hexane, methanol and chloroform) before or after dispersion in water/methanol with the aid of a probe or bath sonication [8,9,11,19,20]. This step is often necessary when NPs' size separation is performed before the detection. It is also possible to only disperse the cream sample in water and NPs are analyzed after dilution [11,17,18]. Different studies are also available for the analysis of TiO_2 NPs in commercial food products such as cakes, candies, chewing gum, wheat flour, sugar glass, coffee cream, confectionary products, cookies, semolina and pasta [9,21–25]. Sample preparation procedures involve several steps in order to release NPs from the sample, such as matrix destruction, extraction and/or purification. For example, the addition of H_2O_2 [21] or H_2O_2/HNO_3 [22] and heating enable the destruction of the organic matrix of the food sample and the separation of TiO_2 NPs from the larger particles. In other samples, such as chewing gum, extraction of TiO_2 NPs from the matrix consists of water extraction, centrifugation and washing steps [23]. Enzymatic digestion has been applied to seed samples by adding α-amylase for carbohydrate degradation after protein destruction with a Tris buffer [25].

A wide range of techniques is available for NPs' characterization, including microscopy, spectroscopy and size separation techniques. Traditionally, microscopy-based techniques (Transmission Electron Microscopy (TEM) and Scanning Electron Microscopy (SEM)) provide information about the size and shape of NPs, and also on the elemental composition after coupling with Energy Dispersive X-Ray Fluorescence Spectrometry (EDXRF). Light Scattering methods, including Dynamic Light Scattering (DLS) based on the diffusion rate of particles and Multi Angle Light Scattering (MALS) based on the angular dependence of light scattering are also available. Information about the hydrodynamic diameter (D_h) and the gyration diameter (D_g) of NPs can be obtained. Among these techniques, DLS is commonly used due to its simple operation and rapid analysis, but an overestimation of particle size may result when small and large particles and their aggregates co-exist in a sample [26]. MALS is often used as a detector after size fractionation of particles by Flow Field-Flow Fractionation techniques (FFF) [27]. These techniques can also be hyphenated to ICP-MS to obtain information about the NPs composition. More recently, Single-Particle Inductively Coupled Plasma Mass Spectrometry (spICP-MS) has been used to quantify the particle concentration and size, assuming spherical particles, by means of the frequency of analytical signals and the relationship between mass and density, respectively [28]. This technique is gaining more and more importance, especially on a routine basis due to its specificity and rapidity [29,30].

In research studies of NPs analysis, the procedures are very time consuming, instruments are often expensive and data treatment is intensive. However, in future years, qualitative characterization of NPs will be part of quality control processes both at industry and institution levels in order to provide a rapid decision of the presence/absence of NPs. Therefore, the current research methodologies need to be adapted to fast and relatively cheap studies considering the perspective towards routine analysis. In fact, the analysis of NPs will require fast screening tests. Thus, the future methodologies will encompass fast, robust, reliable, automated, properly validated procedures, easy-to-use, integrated analytical techniques, etc., as in other routine analysis [31].

In this work, several potential techniques have been assessed on a routine basis for the analysis of TiO_2 NPs. These techniques were commonly used in several research papers. However, an evaluation of their characteristics and requirements have not been yet performed in terms of their implementation in routine analytical laboratories. Some steps such as, the instrument performance, the utilization of relevant tests to ensure the regular working of the instrument, the use of reference materials to check accuracy of the whole analytical process and the study of the repeatability were considered in this work. In order to perform this evaluation and to select the potential techniques more suitable for routine analysis of NPs, the presence of TiO_2 NPs was studied in two consumer products (sunscreen and sugar-coated chocolate candies) using several techniques. DLS and spICP-MS were selected due to their expected easy implementation making them adapted for this objective. AF4-MALS-ICP-MS was selected since it is considered as a reference technique for NPs characterization even if the measurement takes a long time. Microscopy techniques (SEM and TEM) were also used as complementary techniques to confirm the results.

2. Experimental

2.1. Instrumentation

Dynamic Light Scattering (DLS) analyses were performed using a Cordouan Technology VASCO-2 particle size analyzer (Cordouan Technology, Pessac, France) in combination with the software nanoQ v2.

The NexION 300X ICP-MS fitted with a Meinhard nebulizer and a cyclonic spray chamber was used for the analysis of TiO_2 NPs' nanodispersions (without previous separation) according to two modes of operation: a standard one (without reaction gas supply into the cell), and with the collision cell filled with He (Perkin-Elmer, Shelton, CT, USA) for the determination of total Ti content. It was also employed operating in the single particle mode using the Syngistix™ Nano Application Module 1.0 (Perkin-Elmer, Shelton, CT, USA) for nanodispersions analysis.

The Asymmetric Flow Field-Flow Fractionation (AF4) system employed for NPs size separation consists of an Eclipse® (Wyatt Technology, Santa Barbara, CA, USA) using a long channel (275 mm length) and a regenerated cellulose (RC) membrane with a 10 kDa cut-off (Wyatt Technology). The detection chain contains a UV–Vis detector operating at 240 nm (VWD, 1200 series, Agilent Technologies) and a Multi Angle Light Scattering (MALS) detector of 18 angles operating at 663.9 nm (DAWN HELEOS II, Wyatt Technology). Data from the different detectors were collected and treated with the Astra 6.0.2.9 software (Wyatt Technology). The chemical composition of particles eluted from AF4-MALS (particle fractionation) was obtained by coupling AF4-MALS to the Agilent 7500cx ICP-MS (Agilent Technology Ltd., Japan) fitted with a Micromist nebulizer and a Scott spray chamber. The ICP-MS was used according to two modes of operation: a standard one (without reaction gas supply into the cell), and with the cell filled with He. Additionally, the spICP-MS Agilent 7900 ICP-MS (Agilent Technology Ltd., Japan) was used for the analysis of particles eluted from AF4-MALS particle fractionation. This instrument was fitted with a Micromist nebulizer, a Scott spray chamber and with the Single Nanoparticle Application Module for ICP-MS Mass Hunter software (G5714A). These analyses were performed using the collision cell filled with He.

Micrographs were taken with a LVEM5 (Delong Instrument, Brno, Czech Republic), a low-voltage table-sized electron microscope operating both in transmission mode (TEM) and scanning mode (SEM) without requirement of dark room or cooling water. This instrument used a Schottky field emission gun at a nominal acceleration voltage of 5 kV and the SEM mode was obtained using back scattered electrons detectors (BSE detection). Image J software was employed for microscopy data treatment [32].

A hot block digestion system (SCP Sciences, Courtaboeuf, France) and an ultrasonic bath model 5510 (Branson, Switzerland) were used for sample preparation prior to total element determination and extraction of TiO_2 NPs (500 W, 20% power), respectively. Separation of the solid sample from the liquid fraction after defatting with hexane was performed with a model Rotofix 32A centrifuge (Hettich, Marne la

Table 1
Standard nanoparticles used for optimization/calibration/validation experiments.

Nanoparticles	Diameter (nm)	Concentration	Additional information	Use
Polystyrene	46 ± 2 102 ± 3 203 ± 5	1 g polymer/100 g	Standard suspensions (Thermo-Scientific, Waltham, USA)	Optimization (DLS, AF4-MALS) Calibration (AF4-MALS)
Gold	30	50 mg/L Au $2.04 \cdot 10^{11}$ NP/mL	Spherical suspensions (50 mg/L) of gold colloid with capping agent of nanopartz carboxylic acid (Perkin Elmer, Concord, Canada)	Calibration (spICP-MS) Optimization (all techniques)
	50	50 mg/L Au $4.48 \cdot 10^{11}$ NP/mL		
	100	50 mg/L Au $5.71 \cdot 10^{11}$ NP/mL		
	10 (TEM, 8.9 ± 0.1)	51.56 ± 0.23 μg/g Au $7.24 \cdot 10^{12}$ NP/mL	Reference materials: RM 8011, RM 8012 and RM 8013, respectively (NIST, Gaithersburg, USA)	Validation (all techniques)
	30 (TEM, 27.6 ± 2.1)	48.17 ± 0.33 μg/g Au $2.27 \cdot 10^{11}$ NP/mL		
	60 (TEM, 56.0 ± 0.5)	51.86 ± 0.64 μg/g Au $2.92 \cdot 10^{10}$ NP/mL		
Titanium dioxide	21	Nanopowder	Sigma-Aldrich (Saint Quentin Fallavier, France)	Optimization (all techniques), used as suspension in water or methanol.
	19 ± 2 (anatase) 37 ± 6 (rutile) 112 ± 4 DLS[a]	Nanopowder	Standard reference material: SRM 1898 (NIST, Gaithersburg, USA)	Validation (all techniques) used as suspensions in water.

[a] Information extracted from the certificate using deionized water, 10 mg/mL of TiO_2 in a suspension using an ultrasonic probe and 50 W power, sonication 15 min at 80% pulsed operation mode.

Vallée, France).

Amicon® Ultra-4 centrifugal filter devices containing a filter device with a membrane of 10-kDa cutoff (Millipore, Saint-Quentin, France) were used for centrifugal ultrafiltration prior to total element analysis.

2.2. Reagents and standards

Multi-elemental stock standard solutions for trace analysis containing 100 mg/L of Ti (CCS-5) and 100 mg/L of Au (CCS-2) were used for elemental calibration (Analab, Bischeim, France).

Nanoparticle standards (polystyrene, Au and TiO_2) were used for optimization, calibration and validation of the methods (Table 1). Due to the lack of suitable reference materials representing nanodispersions of TiO_2 certified on size and of different diameters, two materials of TiO_2 NPs in the form of nanopowders were tested. However, several researchs showed that food-grade TiO_2, cosmetic TiO_2 and available TiO_2 standards presented different properties in terms of particle size, coating, particle surface, presence of other different elements (P, Al, Si), specific surface area, toxicity and crystal phase [33–37]. Thus, these materials are not completely representative of the TiO_2 present in consumer products.

Sample digestion was performed with analytical reagent-graded HNO_3 67% w/w (VWR Prolabo, Fontenay-sous-bois, France), H_2O_2 30% w/w (VWR Prolabo, Fontenay-sous-bois, France) and HF 40% w/w (Baker-Instra, Center Valley, USA). Hexane (> 99%, Sigma-Aldrich, Steinheim, Germany) was used for sample defatting. Ultrapure water obtained from a Milli-Q system (Millipore, Bedford, USA) was used for all sample preparations and analysis.

2.3. Samples

Two everyday products containing TiO_2 were analyzed by several techniques, a sunscreen (emulsion) and chocolate candies (solid). They were purchased from local supermarkets (Pau, France). The sunscreen SPF 30 (as cream) contains TiO_2/TiO_2 (nano) as written on the label, other present components are iron oxides, dimethicone and aluminum hydroxide. The colorful sugar-coated chocolate candies also contain TiO_2 as a food additive (E171 on the label). These samples consist of a piece of chocolate, with a candy shell where TiO_2 is present. Other mentioned additives are E100 (curcumin), E120 (carmine), E133 (brilliant blue), E160a (provitamin A) and E160e (beta-apo-8′-carotenal (C30)).

2.4. Sample preparation

The different procedures applied in this study are summarized in Fig. S1 (Appendix).

2.4.1. Sample preparation for NPs characterization

2.4.1.1. Sunscreen. The procedure used for TiO_2 NPs determination in sunscreen was adapted from the literature [9,11,19]. A defatting step was first applied by adding 10 mL of hexane to 0.1–0.5 g of sunscreen sample. After shaking (1 min) and sonication (30 min), the mixture was allowed to settle for 1 h and centrifuged (5 min, 3000 rpm). The hexane supernatant phase containing fat was removed. Finally, 19.5 mL of water and 0.5 mL of hexane were added to the solid residue and resuspended by shaking (1 min) and sonication (30 min). Finally, the sample was filtrated (0.45 μm) to remove large particle aggregates.

2.4.1.2. Sugar-coated chocolate candies. TiO_2 of this sample is mainly present in the coating of candies, thus only this part was considered in this study. Extraction was performed by adding 4 mL of ultrapure water to eight candies (around 7 g), the mixture was manually shaken for 1 min (until complete extraction of the coating in the aqueous suspension) and the chocolate core was removed. Then, ultrapure water was added up to 20 mL and the suspension was sonicated for 30 min to disaggregate the particles and to assure a homogeneous suspension before analysis. Finally, the aqueous extract was filtrated (0.45 μm).

The filtration step (0.45 μm) was performed to remove large aggregates before the analysis and because it was reported that colloids present in a sample can be operationally defined as passing a 0.45 μm filter but remaining retained by a 1 kDa ultrafiltration membrane [38]. However, filtration may also prevent the analysis of NPs higher than approximately 350 nm as reported elsewhere [39]. In the literature, samples extracts containing NPs were submitted to centrifugal ultrafiltration to evaluate the dissolved fraction that passed the (10 kDa) membrane [40]. For both samples, 2 mL of extracts were also submitted to ultrafiltration centrifugation for 90 min at 3000 rpm using Amicon® vials containing a 10 kDa ultrafiltration membrane. The final ultrafiltrated volume obtained (0.5 mL) was analyzed by ICP-MS to estimate the dissolved Ti content.

2.4.2. Total Ti determination by ICP-MS

Total Ti content present in the sunscreen and in the coating of chocolate candies was determined after acid digestion. Briefly, 0.1 g of sunscreen or 1 mL of the coating water extract were digested with 2.5 mL HNO_3, 2.5 mL H_2O_2 and 0.5 mL HF using the following temperature program: up to 45 °C in 15 min, stabilization at 45 °C for 60 min, up to 90 °C in 15 min, and stabilization at 90 °C for 180 min. Ultrapure water was added up to 30 mL to decrease the acid concentration in the liquid sample before ICP-MS analysis. Isotopes 47 and 48 were used for quantification. Same digestion protocol was used for total Ti determination in both filtrated and ultrafiltrated extracts.

2.5. Description of NPs measurements

In this section, in addition to the analysis of nanodispersions obtained from the two samples studied, relevant tests related to ensure the regular working of the instruments, the use of standard nanodispersions to demonstrate the general instrument performance, as well as the use of reference materials were also described to prove the accuracy and precision of the methodology.

2.5.1. DLS measurements

DLS measurements were performed with a 65 mW laser (657 nm wavelength) at a temperature of 25 °C. A solvent refractive index of 1.33 was used since the major component is water. This value was also selected when hexane was present because their refractive indexes values were very similar (1.37). A refractive index value of 1.56 was used for the material and selected as a compromise because of the multiple sample matrix components as previously commented elsewhere [41]. One drop of sample suspension was deposited onto the sample cell and irradiated by a laser. The autocorrelation function (ACF) of the scattered light intensity corresponded to the average of 10 consecutive acquisitions of 30 s each. The number of channels and the time intervals were adjusted for each sample. Each acquisition was processed using both the Padé-Laplace inversion algorithm and the Cumulants method. Intensity based size was converted to number average size in order to compare results with the EC recommended definition of nanomaterial.

As advised by the manufacturer, Au NPs' standards were directly analyzed and polystyrene nanosphere standards were diluted in ultrapure water to obtain a concentration of 50 μg/g before DLS analysis. TiO_2 nanodispersions were analyzed after dispersion of the two nanopowder materials in water or methanol aided by bath and/or probe sonication.

Quality control of DLS measurements was daily performed by analysis of a 100 nm polystyrene nanospheres suspension (Table 1).

2.5.2. spICP-MS measurements

spICP-MS enables the simultaneous determination of both dissolved metal concentrations and NPs' characterization (concentration, size and size distribution). An important parameter to calculate for spICP-MS analysis is the transport efficiency (TE). TE is related to the efficiency of the sample delivery taking into account losses due to sampling and nebulization and the differences between the ion transmission in the case of NPs and dissolved elements following the particle number method [42]. This method was also utilized in recent studies, where TE was calculated using NPs of Au and Ag for further analysis of TiO_2 NPs [43,44]. TE can be used for converting the particle net area intensity data into size information through a mass flux calibration curve.

According to the recommendations of the manufacturer, a particle size and a dissolved calibration were performed daily to measure the TE in the NexION ICP-MS instrument. The dissolved calibration was performed using Au standards between 1 and 10 μg/L. Particle size calibration was performed using 30, 50 and 100 nm Au NPs dissolved in ultrapure water to obtain a concentration of particles of approximately 200,000 particles/mL as recommended by the manufacturer. TE was then calculated from the ratio between both calibration slopes, being 6.7–10.5% in these analyses.

For TiO_2 NPs determination in real samples, a calibration of dissolved Ti was performed at concentrations in the range 1–50 μg/L to relate the signal intensity with the mass concentration (μg). Then, the TE obtained before was applied for TiO_2 NPs analysis taking into account the density of TiO_2 (4.23 g/cm^3) and the mass fraction of Ti in the compound TiO_2 (60%). Samples were analyzed after filtration and dilution to obtain a particle concentration in the range of 100,000–250,000 particles/mL. Ti was determined considering a m/z ratio of 48, a dwell time of 100 μs and a data acquisition time of 100 s. Lognormal fitting function was directly used from the software provided by the manufacturer.

The nebulization efficiency in the Agilent 7900 ICP-MS for spICP-MS analysis was evaluated according to the recommendations of the manufacturer using only one dissolved standard of Au at 1 μg/L and one nanodispersion of Au NPs of 56 nm (RM 8013) at a concentration of 50 ng/L. Here, nebulization efficiency corresponded to the ratio of the observed number of particles to the calculated number of particles (a value of 0.056 was obtained). The selected parameters were a sample inlet flow of 0.346 mL/min using a peristaltic pump, a dwell time of 100 μs and an acquisition time of 60 s.

2.5.3. AF4-MALS and AF4-MALS-(sp)ICP-MS measurements

According to the literature [8,9,19] and preliminary experiments, conditions used for AF4 separation were: a regenerated cellulose (RC) membrane with a 10 kDa cut-off (Wyatt Technology), a 350 μm spacer, and measurements were performed at a cross flow of 0 and 0.5 mL/min. The elution program applied was the following. An elution step at 0.5 mL/min was first used to clean and prepare the channel (2 min). An injection of the sample is then performed (focus + injection, 5 min) followed by a focus step (5 min) in order to concentrate the sample at the entrance of the channel prior to the analysis (injection flow 0.2 mL/min and focus flow 1.5 mL/min). Then, an elution flow of 0.5 mL/min, as well as a cross-flow of 0.5 mL/min were applied and were kept constant for 60 min. Finally, the cross-flow was stopped; and the elution and injection flows were applied to allow elution of the residues present in the channel (5 min). Ultrapure water was used as the mobile phase for the analysis of standards and reference materials. For real samples, two different mobile phases were tested (ultrapure water and SDS 0.1% w/v) to evaluate the influence of the mobile phase in the interactions of particles with the membrane.

MALS detector gives an absolute determination of particle size based on the angular dependence of the scattered light. The particle size is defined by the gyration diameter also called root mean square diameter (D_g = 2 × root mean square radius, rms) corresponding to the slope of Debye plot using the Zimm formalism.

Based on the diffusion of particles into the AF4 channel, calibration to convert AF4 retention time into hydrodynamic diameter (D_h) was daily performed using suspensions of polystyrene nanospheres in a concentration of 50 μg/g prepared from the stock nanodispersions described in Table 1. Volumes of 50, 20 and 10 μL of nanosphere suspensions with sizes of 46, 102 and 203 nm were respectively injected to obtain an optimal signal.

Nanostandards of Au were analyzed without any preparation. In particular, 50 μL of 30 nm and 50 nm, and 10 μL of 100 nm of the original nanodispersions were injected as three independent analyses. In that case, the amount of Au retained in the membrane was calculated by coupling the natural outlet flow rate from AF4 to the ICP-MS.

For real sample analysis, the volume injected was 10 μL and elution conditions were the same as described before.

The coupling of AF4 to MALS provided information of intensity-based size distribution, but when coupled to ICP-MS, the information obtained was mass-based signal. In order to compare the number of particles obtained by the different detectors, the mass-based signal was converted to number-based size distributions using the method

described in Peters et al. [21].

For the AF4-MALS-spICP-MS on-line analysis, the light scattering detector was directly coupled to the ICP-MS, and the single particle mode was programmed to analyze the sample flow every minute for 40 min. In the same way, injections of 10 μL of each sample (sunscreen and chocolate candies) without dilution or previously diluted ten times were performed to evaluate if the dissolved Ti concentration affected the particle size determination and counting of the number of particles.

Unless stated otherwise, results based on repeated measurements are expressed as x ± σ, where x is the mean of three individual analyses and σ the standard deviation between these values.

2.5.4. TEM and SEM measurements

The LVEM5 microscope is especially suitable for routine analysis because it is a compact benchtop version that does not require a dark room or cooling water. This microscope provides an easy service and can work in TEM or SEM mode at a moderate price in comparison with other instruments.

Chocolate candies and sunscreen extracts analyzed by microscopy techniques were prepared by directly placing 5 μL of suspension on 300 mesh ultrathin carbon film copper grids (Cu300-HD, Pacific Grid Tech) previously treated by glow discharge using an ELMO system (Cordouan Technologies, Pessac, France) and making the carbon membrane hydrophilic. After removing the excess of water using a flat filter paper, the TEM grids were air-dried at room temperature for 10 min prior to analysis.

Chocolate candies extract used for SEM analysis was prepared by centrifuging the suspension at 3000 rpm for 10 min. The sedimentary phase was then collected and air-dried at room temperature for 12 h. The powder was finally stuck on the copper SEM stub using double-sided carbon tape.

3. Results and discussion

3.1. Performances of characterization techniques

Before characterization of NPs in consumer products, each methodology has been optimized and validated using the different standards and reference materials of NPs presented in Table 1. As commented before, and due to the lack of nanodispersions of certified reference materials of TiO_2 NPs of different sizes, instrument performance and methodology has been checked using Au nanodispersions, polystyrene nanodispersions and TiO_2 nanopowder dispersed in water/methanol.

3.1.1. DLS performances

DLS analysis of NPs standards was performed considering two modes of calculation, the Cumulants and the Padé-Laplace models. Results summarized in Table 2 showed that the mean diameter in number-based size distribution was in accordance with reference or certified values for Au NPs and polystyrene nanospheres applying both models, with some exceptions, demonstrating the relative low effect of particle refractive index on the determination of the number-based size distribution. The Cumulants method did not work properly for Au 100 nm and to a lesser extent for polystyrene 200 nm because samples presented high polydispersity (0.25 in case of Au) and it was thus recommended to use the Padé-Laplace model in that case. The Au 100 nm nanodispersion was also not sufficiently diluted and thus particle interactions and multiple scattering effects probably decreased the measured diameter [45]. On the contrary, for the 50 nm Au nanodispersion, the Padé-Laplace model provided a smaller diameter than expected. Nevertheless, considering the mean size based on intensity distribution for this standard, the obtained diameters were similar for the two models (65 ± 2 nm and 67 ± 2 nm for Padé Laplace and Cumulants, respectively). Consequently, a considerable amount of particles with a diameter around 11 nm shifted the mean size based on number distribution to small values.

DLS analyses were performed for TiO_2 nanodispersions prepared from the commercial nanopowder (Sigma-Aldrich) dispersed in water or methanol. Aggregation was observed since the two models showed higher size values than expected (Table 2). Aggregation and agglomeration were also observed in reported studies for the analysis of TiO_2 NPs obtained from nanopowders dispersed in water [46–48]. The provider declared that even with a primary size of about 21 nm, the particles of this material appeared as agglomerates with a size < 150 nm [47]. For this TiO_2 material and others of similar primary size such as Aeroxide® P25 of 25 nm, the size obtained in different studies by DLS [47], AF4-MALS [47] and TEM [48] were 70–100 nm, 49–87 nm and 25–85 nm, respectively. Even so, other authors found aggregates of 100–600 nm [11] by AF4-MALS-ICP-MS. Larue et al. [49] obtained by TEM a diameter of 217 ± 37 nm and 197 ± 11 nm instead of 4 nm and 150 nm, respectively. The high range of aggregation could be attributed to the use of ultrasonic bath for the preparation of the suspension. However, probe sonication also tested in this work did not improve the results as already observed in reported studies [46].

The results obtained demonstrated the ability of DLS for a simple and fast sample screening. However many differences could occur depending on the selected model especially for polydisperse samples. Therefore, DLS should be considered as a technique that enables fast measurements to evaluate the efficiency of the sample preparation step and/or stability of the suspension rather than an accurate quantitative technique.

3.1.2. spICP-MS performances

spICP-MS performance was assessed by the determination of the

Table 2
Results obtained by DLS, spICP-MS and AF4-MALS-ICP-MS for NPs determination in different standard nanodispersions.

Reference or certified value (nm)	DLS			spICP-MS	AF4-MALS
	Mean diameter in number-based size distribution D_h (nm)		Polydispersity index	Mean diameter (dense core) (nm)	Mean diameter D_g (nm)[a]
	Cumulants model	Padé-Laplace model			
Au: 30 nm	30.9 ± 3	26 ± 8	0.15	31 ± 1	–
Au: 50 nm	43 ± 2	12.4 ± 0.4	0.15	47 ± 1	–
Au: 100 nm	65 ± 5	106 ± 2	0.25	98 ± 2	–
Polystyrene: 46 ± 2 nm	45 ± 9	43 ± 8	0.1	–	49 ± 4
Polystyrene: 102 ± 3 nm	116 ± 6	112 ± 2	0.01	–	100 ± 3
Polystyrene: 203 ± 5 nm	168 ± 1	212 ± 34	0.1	–	193 ± 10
TiO_2 ≈ 21 nm (in methanol)	215 ± 5	204 ± 5	0.03	–	–
TiO_2 ≈ 21 nm (in water)	274 ± 33	272 ± 20	0.03	106 ± 3	18 ± 2

x ± σ, where x is the mean of three individual analysis and σ the standard deviation between these values.
TiO_2 from Sigma-Aldrich.
[a] Sphere model by MALS, D_g corresponds to the geometrical diameter of the polystyrene nanospheres.

particle size of Au NPs in the three individual standard nanodispersions and in a mixture combining these nanodispersions. Concerning monodisperse samples, results given in Table 2 were very close to reference values whatever the size was. For the polydisperse sample containing a mixture of these three sizes, the obtained mean diameters were 36.0 ± 0.4 nm, 46 ± 3 nm and 93 ± 3 nm, being also in accordance. This technique was thus able to discriminate NPs of different sizes in the same nanodispersion. For TiO_2 dispersion prepared from the nanopowder (Sigma-Aldrich), most frequent size (63 ± 4 nm) and mean diameter (106 ± 3 nm) were higher than the reference value as already observed by DLS. Thus, spICP-MS results also showed aggregation of particles (Table 2).

3.1.3. AF4-MALS and AF4-MALS-ICP-MS performances

Particle size calibration was based on the AF4 theory, that is, the separation of particles by their diffusion coefficient. Because no well-characterized TiO_2 particles were available for calibration purposes [44], NPs of a different composition were used. Indeed, AF4-MALS calibration to convert retention time into hydrodynamic diameter is generally performed with standards of polystyrene [47,50]. Considering the weak interaction of particles with the membrane, the relation can be further applied to NPs having a different composition. In order to check if the response is the same whatever the nature of the NPs is, calibration was performed using polystyrene nanospheres and Au NPs in the same elution conditions. This experiment showed that the time of retention for Au NPs or polystyrene nanospheres having a similar size was not the same, resulting in a different slope of the calibration curve (Fig. S2 (Appendix)). This was particularly true with an already used membrane (≈ 20 injections). Interactions could then occur between particles or with the membrane when an already used membrane was utilized. The total amount of injected Au considering the injected volume and the concentration of nanodispersions (2.5, 2.5 and 0.5 μg of Au for 30, 50 and 100 nm, respectively) and the total content of Au eluted and quantified by online AF4-ICP-MS (determined by ICP-MS after external calibration, 0.17 μg, 0.2 μg and 0.17 μg, respectively) were compared using a new membrane. Low recoveries were obtained (7%, 8% and 34% for 30, 50 and 100 nm, respectively) confirming that a large amount of Au NPs is trapped on the membrane and negatively affected or disturbed the following analyses as it was observed with the used membrane. Fig. S3 (Appendix) includes an image of the membrane colored pink due to the adsorption of Au NPs. Retention time of particles of a given dimension is in theory independent of their density and chemical nature, calibration could be therefore performed with any kind of spherical particles [50,51]. But in practice, the way the particles are capped/stabilized (e.g. citrate, PVP, carboxylic acid) can influence interaction of particles with the membrane and consequently, the retention time. Gigault et al. compared the behavior of four NPs' populations with similar nominal size and different nature (Ag, Au, Se and polystyrene nanospheres) during AF4 separation [50]. They concluded that there existed a clear influence on the composition of the particles, compromising thus the effectiveness and accuracy of using only polystyrene beads to calibrate retention time of particles of different nature. Geiss et al. studied size-calibration with polystyrene nanospheres for Ag NPs analysis and observed very large differences in retention times due to particles-membrane interaction [51]. These discrepancies with the nature of NPs can be interpreted as distinct surface chemistry of the particles or differences in the attractive van der Waals forces between the NPs and the accumulation wall (membrane surface) [50,51].

Thus, to minimize the deviation that could occur between samples and standards, the calibration must be performed daily with standards having physico-chemical properties close to the nature of the NPs present in the sample.

The AF4-MALS analysis of TiO_2 NPs showed the absence of signal for filtrated nanodispersion probably because of the formation of large aggregates that remained in the filter. However, the unfiltrated TiO_2 nanodispersion showed a very thin peak (t_r 14.5 min), which after the polystyrene nanospheres calibration attained a D_h accordant with the reference value (Table 2). The coupling of AF4 to ICP-MS showed that this MALS signal corresponded to Ti.

The size of the particles can also be defined as the gyration diameter (D_g) instead of the hydrodynamic diameter using MALS data without any particle size calibration. In that case, the absolute size is related to the mass distribution of the particle with respect to its center of gravity. Results obtained for polystyrene nanospheres were in accordance with the indicative values regardless of the size (Table 2). However, MALS could not be applied for sizing Au NPs because at the laser wavelength used (663 nm), Au NPs exhibited strong plasma resonance and disturbed the typical size dependent angular dispersion and impeded the capacity to obtain absolute size information (D_g) by MALS detection [52,53]. This is also the case for some other metallic NPs such as Ag [52,53]. Therefore, the direct absolute determination of size by static light scattering techniques has some limitations, especially for metallic NPs. In that case, a characterization based on the retention time with appropriate standards is also needed.

3.1.4. Analytical figures of merit

Analytical parameters and accuracy of the three previously optimized techniques were evaluated for Au (RM8011, RM8012 and RM8013) and TiO_2 (SRM 1898) NPs reference materials.

For DLS and AF4-MALS, theoretical values of size detection limit (D_{min}) were 10 nm. However, the presence of large particles in the sample could increase considerably this limit especially for DLS since a separation step was not applied. The analysis of reference materials confirmed that these two techniques were able to determine a size of 10 nm with good accuracy and repeatability (Table 3). The D_{min} in spICP-MS was calculated considering the 3-σ criterion being 18 nm for Au NPs and 32 nm for TiO_2. These results accorded with D_{min} values reported in the literature (10–25 nm for Au [54–56] and 20–80 nm for TiO_2 [54,57]). From those results, the less sensitive technique in terms of diameter was spICP-MS, but this method was the most sensitive in terms of particle concentration. Concentrations of 5 ng/L of 30 nm Au NPs were detected by spICP-MS, whereas 50 μg/L were required for AF4 and DLS for the same order of NPs size (more information in Table S4 (Appendix)).

Repeatability (n = 3) and reproducibility (n = 5), estimated as between-day relative standard deviation (% RSD), were below 6% and 14%, respectively, suggesting that spICP-MS had a satisfactory precision.

Concerning the accuracy of DLS (Table 3), satisfactory results were attained for Au NPs using both models, but the Pade-Laplace seemed more appropriate for the smallest particles. Analysis of the RM 8011 sample was not possible by spICP-MS because the size was lower than the D_{min}. For RM 8012 and RM 8013, the diameters obtained were in accordance with the values given in the certificate both in terms of most frequent and mean size. The aggregation of TiO_2 NPs did not allow obtaining good results for SRM 1898 by DLS because the D_h was approx. 200 nm, higher than the primary particle size. However, the most frequent size obtained by spICP-MS was close to the certified values for rutile (37 nm) but the determination of the particles having a size of 19 nm (anatase) was not possible because this value was very close to D_{min} of the technique. The problem of aggregation was even informed in the certification report of SRM 1898, where it was indicated that after dispersion of the particles in water by means of a probe sonication for 15 min, DLS analysis provided a size in the range of 68–151 nm [58]. According to the certificate, large aggregates were present, especially for non-sonicated suspension or dispersions sonicated with an ultrasonic bath as is the case here [58].

For AF4-MALS-ICP-MS, Table 3 presents results obtained with the two calibration modes (polystyrene and Au NPs). As expected, a calibration with Au NPs provided better accuracy with the values given in the certificate (86 and 97% for 30 and 60 nm, respectively) than calibration with polystyrene (123 and 118%, respectively). The

Table 3
Accuracy obtained by the different techniques for the determination of Au and TiO_2 NPs size in different reference materials.

Certified value (nm)	Found value					
	DLS		spICP-MS		AF4-MALS	
	Mean diameter D_h (nm)		Most frequent diameter (dense core) (nm)	Mean diameter (dense core) (nm)	Calibration PS nanospheres	Calibration Au NPs standard
	Cumulants model	Padé-Laplace model			Mean diameter D_h (nm)	Mean diameter D_h (nm)
RM 8011 (10 nm) - Au SEM: 9.9 ± 0.1 TEM: 8.9 ± 0.1 DLS: 13.5 ± 0.1	35 ± 4	11.9 ± 0.2	< D_{min}	< D_{min}	15 ± 2	6 ± 2
RM 8012 (30 nm) - Au SEM: 26.9 ± 0.1 TEM: 27.6 ± 2.1 DLS: (173°) 28.6 ± 0.9 DLS: (90°) 24.9 ± 1.2	27 ± 2	27 ± 3	22 ± 1	30 ± 1	37.0 ± 0.8	26.9 ± 0.1
RM 8013 (60 nm) - Au SEM: 54.9 ± 0.4 TEM: 56.0 ± 0.5 DLS: (173°) 56.6 ± 1.4 DLS: (90°) 55.3 ± 8.3	50.7 ± 0.9	69.0 ± 0.2	59 ± 1	63 ± 1	70.9 ± 6.7	58.4 ± 0.3
SRM 1898 - Ti XRD: 19 ± 2 (anatase) XRD: 37 ± 6 (rutile) DLS: 112 ± 4	213 ± 4	207 ± 10	43 ± 2	86 ± 13	20 ± 2	–

PS: polystyrene nanospheres - D_{min}: size detection limit.
x ± σ, where x is the mean of three individual analysis and σ the standard deviation between these values.

Table 4
Total Ti content after each sample preparation step for sunscreen and coating of chocolate candies.

Sample preparation step	Sample	Extract		Filtrated extract		Ultrafiltrated extract	
	[Ti] (mg/g)	[Ti] (mg/g)	Recovery[a] (%)	[Ti] (mg/g)	Recovery[a] (%)	[Ti] (mg/g)	Recovery[a] (%)
Sunscreen	13.14 ± 0.06	12.9 ± 0.9	98 ± 7	12.7 ± 0.2	96 ± 2	0.40 ± 0.03	2.8 ± 0.2
Sugar-coated chocolate candies	NA	1.07 ± 0.02	NA	0.12 ± 0.01	11.2 ± 0.9	0.050 ± 0.002	4.9 ± 0.2

NA: not applicable.
x ± σ, where x is the mean of three individual analysis and σ the standard deviation between these values.
[a] Recoveries calculated taking into account total Ti of the extract.

Table 5
Results obtained by spICP-MS and DLS for the determination of TiO_2 NPs in sunscreen and sugar-coated chocolate candies samples.

Sample	Dilution	Most frequent size (nm)	Mean size (nm)	Particle concentration (part./mL)	Dissolved Ti (μg/L)
spICP-MS					
Sunscreen	1:1000	138.9 ± 0.1	155.7 ± 0.4	20,000	31
	1:4000	106 ± 2	121 ± 3	50,000	7
	1:10,000	95.5 ± 0.3	117.3 ± 0.1	136,000	3
	1:30,000	73.8 ± 0.1	86.9 ± 0.6	240,000	0.8
Mean value	1:30,000	70 ± 6	80 ± 10		
Reproducibility (n = 8, %)		8	13		
Sugar-coated chocolate candies	1:4000	147 ± 7	196 ± 1	1,400,000	2
	1:40,000	55.8 ± 0.1	124.4 ± 0.1	530,000	0.2
	1:120,000	55.0 ± 0.8	119.2 ± 0.9	198,000	0.1
Mean value	1:120,000	52 ± 4	122 ± 4		
Reproducibility (n = 8, %)		8	3		

DLS			
	Mean diameter in number-based size distribution D_h (nm) Padé-Laplace model	Mean diameter in number-based size distribution D_h (nm) Cumulants model	Polydispersity index
Sunscreen	109 ± 9	101 ± 5	0.22
Sugar-coated chocolate candies (1:10 dilution)	128 ± 2	194 ± 24	0.23

x ± σ, where x is the mean of three individual analysis and σ the standard deviation between these values.

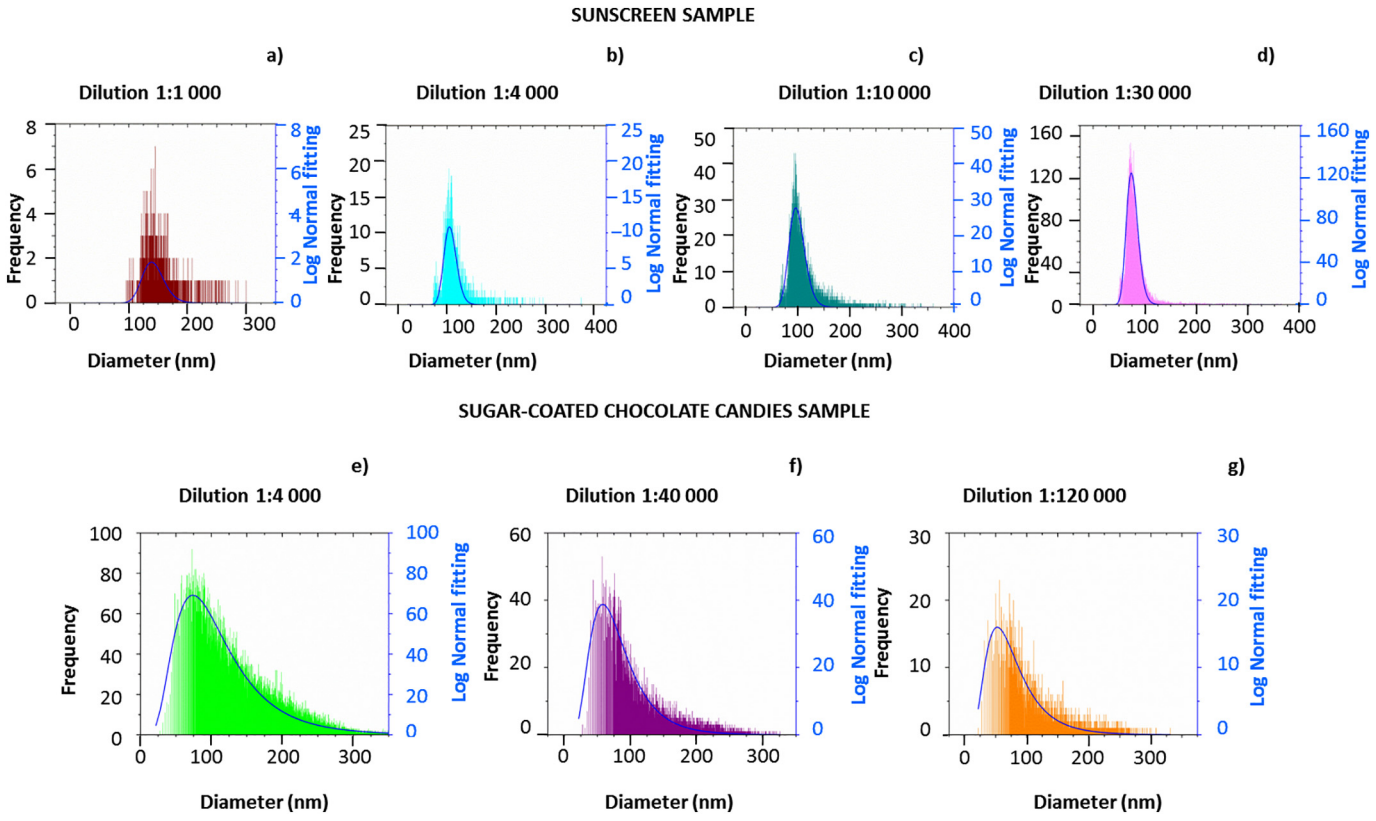

Fig. 1. Histograms obtained by spICP-MS for different dilutions of sunscreen (a–d) and sugar-coated chocolate candies (e–g).

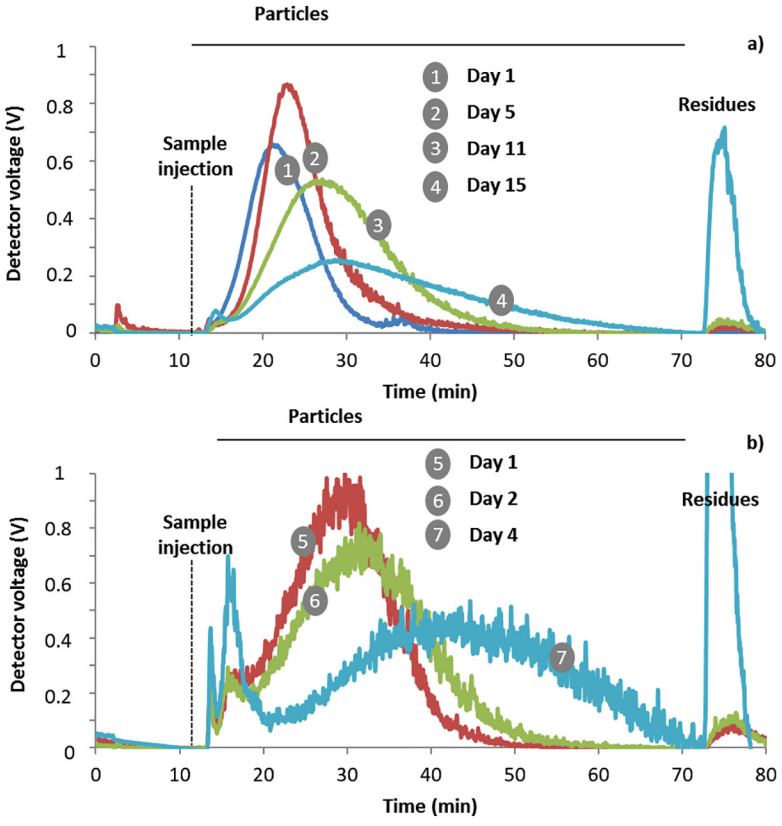

Day	Time (min)	D_h (nm, x±σ, n=3)
1	21.1, 20.0	71 ± 6
5	22.9, 22.0	86 ± 5
11	27.1, 27.5	124 ± 2
15	32.9, 30.0	157 ± 16

Day	Time (min)	D_h (nm, x±σ, n=3)
1	30.6, 29.7	146 ± 5
2	31.4, 35.1	171 ± 20
4	40.5, 50.0	265 ± 53

Fig. 2. Stability of the sample extracts obtained by AF4-MALS for a) sunscreen and b) chocolate candies.

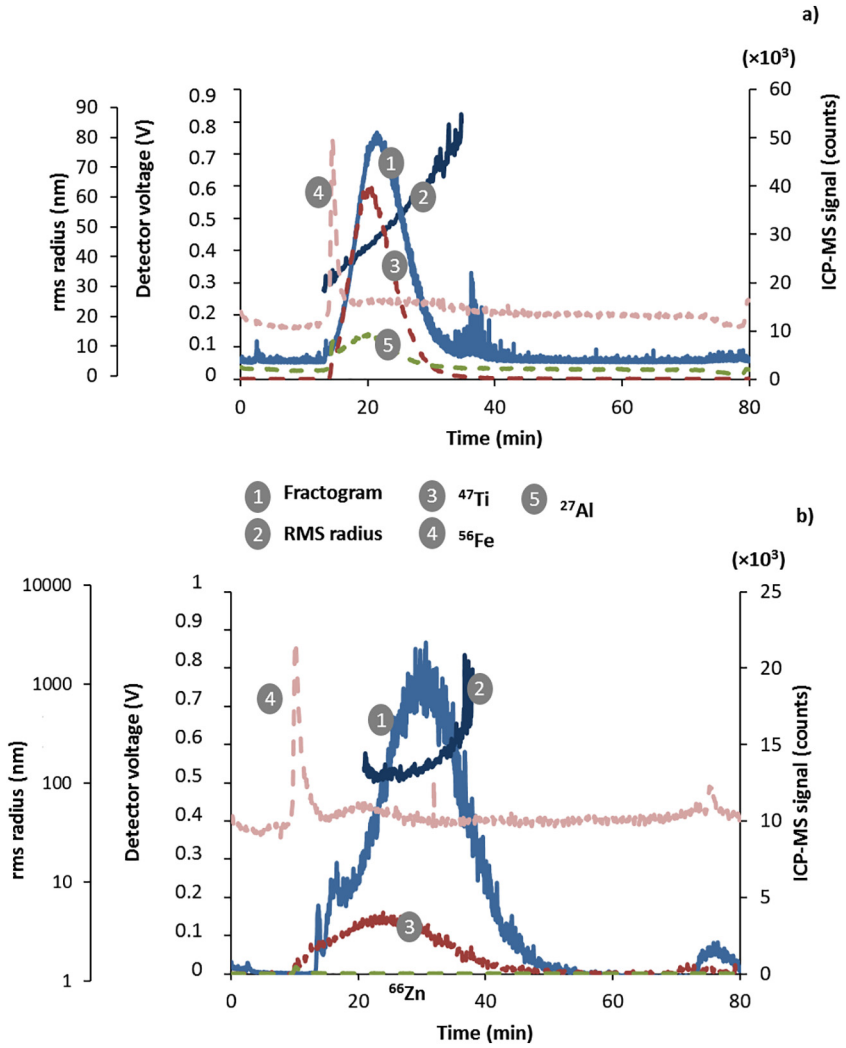

Fig. 3. AF4-MALS-ICP-MS fractograms obtained for a) sunscreen and b) chocolate candies. Fractogram of the two samples are presented, as well as the rms radius (second left vertical axis) and counts of ICP-MS (right vertical axis).

determination of 10 nm NPs was not as accurate because this size was close to the D_{min} of the technique. However, calibration with polystyrene nanospheres seemed suitable for TiO_2 NPs since the size accorded with the reference value given for anatase.

Results obtained from analysis of different NPs' reference materials showed that the three techniques allowed obtaining satisfactory results for Au NPs but some discrepancies were observed for TiO_2 NPs.

3.2. Characterization of NPs in consumer products

The presence of NPs in real samples has been studied by the three techniques previously optimized and compared to microscopy measurements. Studied samples (sunscreen and colored sugar-coated chocolate candies) were characterized after applying the sample preparation procedures presented in Fig. S1 (Appendix).

Before size determination, the Ti content and recoveries were evaluated by ICP-MS at each step of the sample preparation (extraction, filtration and ultrafiltration) after acid digestion. Results summarized in Table 4 showed quantitative recoveries after extraction and filtration for the sunscreen sample, indicating no losses after these treatments. Analysis of the ultrafiltration supernatant, which can be assimilated to the dissolved Ti fraction, showed very low concentration. Thus, Ti in that sample is essentially present as NPs in the extracts and no losses of Ti-containing particles appeared during sample treatment.

In the case of chocolate candies, the low recovery obtained after filtration means that large aggregates containing Ti (larger than 450 nm) were formed. Analysis of the supernatant after ultrafiltration showed that extracted Ti was equally distributed between the supernatant and the NPs' fractions.

As commented above, although standards of TiO_2 were tested, these materials are not very representative of the TiO_2 present in the consumer products because their particles tend to aggregate in water suspension. However, TiO_2, present for example in cosmetics, was reported that the organic components coating the particles (e.g. silicone even a small amount) maintained the water emulsion/suspension very stable [8]. In addition, the organic solvent (i.e. methanol or hexane) used during the sample preparation, reduced the aggregation of NPs due to the formation of a layer on the particle surface and improved the dispersion of NPs in aqueous solution, thus obtaining a lower particle size [59].

3.2.1. spICP-MS and DLS investigations

The results obtained after analysis of the two samples by spICP-MS are presented in Table 5. Histograms are shown in Fig. 1 and indicate a well adjustment of the raw data and lognormal fitting function.

For the sunscreen, a sample dilution between 1:10,000 and 1:30,000 seemed suitable since the number of particles were in the recommended range. The obtained mean size was between 87 and 117 nm for TiO_2

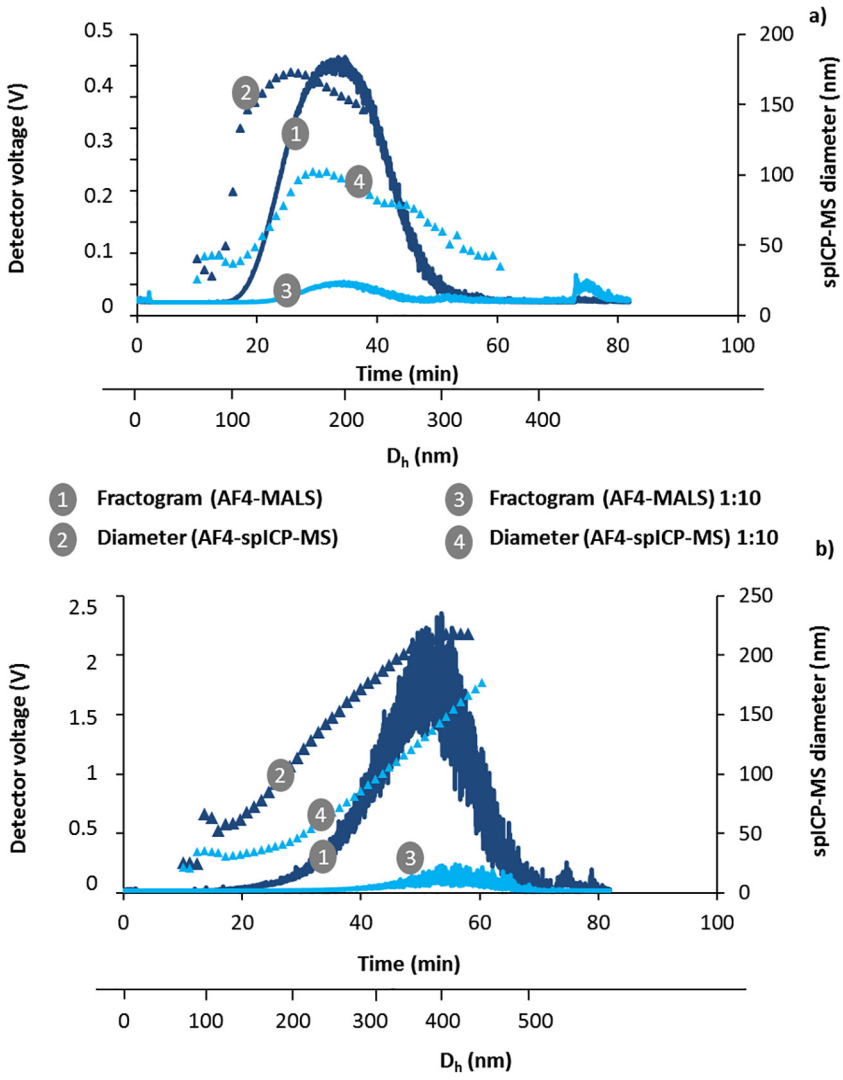

Fig. 4. Representative fractograms obtained by AF4-MALS-spICP-MS for a) sunscreen and b) chocolate candies for undiluted and 1:10 diluted samples.

NPs. As the histograms present a better symmetrical distribution when a 30,000-fold dilution was used (Fig. 1D), this dilution seemed more suitable. The high concentration of ionic Ti hampered the analysis in less diluted extracts due to the high background levels (Fig. 1A-C).

For the sugar-coated chocolate candies, a dilution 1:120,000 was required for TiO_2 NPs determination taking into account the recommended number of particles, but a very similar mean size was also obtained for the 40,000-fold dilution (Fig. 1F). However, an asymmetrical distribution was observed (Fig. 1E-G) showing differences in the most frequent and mean diameters.

Based on these results, dilutions of 30,000 and 120,000 seemed suitable for TiO_2 NPs' size determination in sunscreen and sugar-coated chocolate candies, respectively. In these conditions, the most frequent size and mean size obtained were determined with a good reproducibility (Table 5).

Results obtained by DLS are given in Table 5. For the sunscreen, very similar results were obtained by the two models. Concerning sugar-coated chocolate candies, as the autocorrelation function did not work properly for very concentrated samples because net motion appeared instead of Brownian particle movement [60], a direct analysis of the extracts was rejected. After a 10-fold dilution, the size was reduced using the Padé-Laplace model but not with the Cumulants method. As the PDI was 0.23 and considering that the Padé-Laplace algorithm was better adapted to polydisperse samples, results obtained with this model seemed to be more representative.

3.2.2. AF4-MALS and AF4-MALS-(sp)ICP-MS investigations

In order to improve NPs analysis of real samples by AF4-MALS, different mobile phases were studied (ultrapure water and SDS 0.1% w/v) and obtained fractograms were shown in Fig. S5 (Appendix). Recovery studies of the analytes during fractionation were usually reported in the literature to evaluate potential losses of the sample caused by filtration through the permeation membrane or adsorption phenomena as a consequence of the application of a crossflow (flow across the membrane) [61]. For the evaluation of the recovery rate, sample injections were performed considering peak areas from light scattering and UV signals in absence or presence of a cross-flow of 0.5 mL/min ($R\ (\%) = \frac{S}{S_0} \times 100$, where S is the signal with a cross-flow of 0.5 mL/min and S_0, the signal without cross-flow). The use of these two detectors was recommended in the literature to have a more reliable evaluation [61]. Ultrapure water as the mobile phase provided recoveries for sunscreen and chocolate candies in the range 93–98% for UV detection and 70–80% for MALS. The use of SDS produced a diminution in the recovery in both cases (64–81% for UV detection and 41–75% for MALS). Furthermore, the presence of SDS resulted in a decrease of intensity and the elution of the particles was retarded, thus increasing the analysis time. Additionally, SDS was not generally recommended for ICP-MS due to its detrimental effects on nebulization and transport

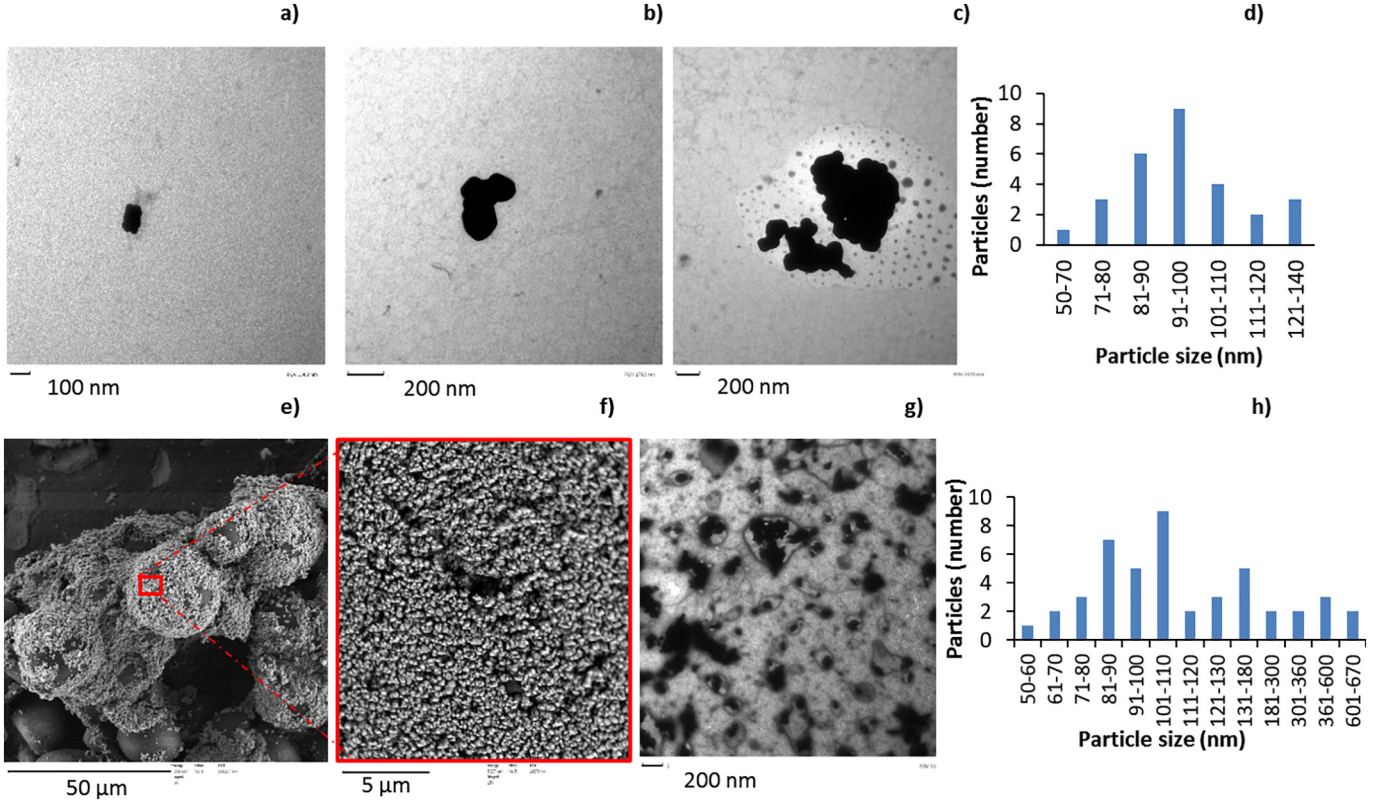

Fig. 5. SEM and TEM images and histograms of chocolate candies (a, b, c, d, e and f) and sunscreen (g and h). a) TEM images of a filtrated extract of chocolate candies. b) and c) TEM images of two aliquots of non filtrated extracts of chocolate candies. d) Histogram of analysis c. e) and f) SEM images of a centrifuged non filtrated extract of chocolate candies. g) TEM image of filtrated extract of sunscreen. h) Histogram of analysis g.

efficiency [62]. Similar results were achieved by Soto-Alvaredo et al. for Sd-FFF, testing different mobile phases [62]. Ultrapure water as the carrier was then selected for NPs analysis in real samples.

Before size determination, the stability of dispersions with time was evaluated for both samples by AF4-MALS. Fractograms are presented in Fig. 2. For the sunscreen, Fig. 2A shows that in the first 5 days after sample preparation, a high and narrow peak was observed with a similar elution time and then similar particle size. After 5 days, this signal became broader, which meant a higher retention time and, as a consequence, a higher particle size due to aggregation or agglomeration. This fact was confirmed by the increase of the peak corresponding to the residues. For the sugar-coated chocolate candies (Fig. 2B), the particles were less stable since they tended to aggregate and agglomerate in a faster way even in 2 days after sample preparation. Therefore, it was recommended to perform analyses as soon as possible after sample preparation. The hydrodynamic diameter (D_h) of the particles was then evaluated using particle size calibration with polystyrene nanospheres since standards of TiO_2 NPs of several sizes were not available. Size distribution was obtained after calculating the size of the particles at the beginning and at the end of the peak. In those conditions, the obtained D_h were close to 80 nm for sunscreen and 150 nm for sugar-coated chocolate candies (Fig. 2). Achieved D_g values were 100 ± 2 nm and 210 ± 26 nm for sunscreen and sugar-coated chocolate candies, respectively.

AF4-MALS was then coupled to ICP-MS and obtained elemental fractograms are presented in Fig. 3. For the sunscreen, Fig. 3A shows the presence of elements at the dissolved state such as Fe which were not retained by the membrane. ICP-MS signals of Ti and Al perfectly overlapped with the peak obtained by AF4-MALS, which meant that the particles contained Ti and Al in their composition. These results confirmed the usual presence of Al in sunscreens because TiO_2 NPs are often coated with a layer of $Al(OH)_3$ to shield against the harmful effects of hydroxyl radicals, superoxide anion radicals and other reactive oxygen species generated when TiO_2 NPs are exposed to UV radiation [63]. For the sugar-coated chocolate candies (Fig. 3B), only Ti was associated to the NPs and we can observe the presence of dissolved Al and Fe.

NPs in the studied samples were also characterized by on-line coupling of AF4-MALS to spICP-MS. The main advantage of this method was the possibility of obtaining the number-based size distribution after particle size fractionation without any mathematical transformation. Nevertheless, interpretation of the results was a difficult task and involved several requirements: a) the performance of AF4-MALS particle size calibration with polystyrene prior to sample injection to obtain hydrodynamic diameter, b) selection of an appropriate dilution for a suitable particle concentration avoiding saturation of MALS detector for achieving gyration diameter and to avoid the detection of two particles at the same time and the saturation of the ICP-MS detector because all detectors were coupled on-line. Additionally, the outlet flow of AF4-MALS was not a very clean system that could have generated the mixture of particles of different sizes at the outlet of the AF4 channel. Moreover, the dissolved ions also interfered in the determination of the number and size of the particles by spICP-MS. It was expected that the coupling AF4-spICP-MS would reduce the dissolved ions, but we can conclude that only at a certain degree, remaining part of dissolved ions retained in the AF4 channel. Furthermore, the dilution rate and injected sample volume were the critical parameters. It was also showed that dissolved ions can interfere in the determination of number and size of particles by spICP-MS [64]. Fig. 4 shows representative fractograms attained by AF4-MALS and AF4-spICP-MS for sunscreen (Fig. 4A) and chocolate candies (Fig. 4B), testing undiluted and diluted samples. These figures also confirmed the presence of Ti-containing NPs in those samples. The mean diameter obtained for the sunscreen sample was 98 ± 6 nm and 79 ± 7 nm for undiluted and diluted sample,

Table 6
Comparison of the main characteristics of the techniques applied in this work for NPs characterization.

Figures of merit	Technique						SEM/TEM
	DLS	AF4-MALS	AF4-MALS-ICP-MS	AF4-MALS-spICP-MS	spICP-MS	ICP-MS	
Price	−	+	++	+++	+	+	+
Availability in the labs	+	−	−	−	+	+	−
Composition information	No	No	Yes	Yes	Yes	Yes	No
Diameter	D_h	D_h, Dg	D_h, Dg	D_h, Dg, mass-based diameter	Mass-based diameter	No	Dense diameter
Size distribution	Yes (number, volume, intensity)	Yes (mass)	Yes (mass)	Yes (number)	Yes (number)	No	Yes (number)
Time of measurement	Few min	Hours	Hours	Hours	Some min	Some min	Some min
Sensitivity	−	+	+	++	++	+	−
LD in size (D_{min})	1 nm	10 nm	10 nm	Depending on the element 10–300 nm	Depending on the element 10–300 nm	No	4 nm SEM 1.5 nm TEM
LD in concentration	μg/L–mg/L	μg/L	μg/L	ng/L	ng/L	ng/L–μg/L	μg/L
LD in particles/mL	10^6–10^{11} NPs/mL	10^8 NPs/mL	−	−	10^3–10^4 NPs/mL	−	10^9–10^{11} NPs/mL
Accuracy	−	+	+	+/−	+/−	+	+
Precision	−	+	+	+/−	+/−	+	−
Benefits	User-friendly Fast screening	Size fractionation	-Size fractionation -Elemental composition	-Size fractionation -Elemental composition -Particle size composition -Removal of dissolved element -Very sensitive	-Size and composition simultaneously -Very sensitive	Very sensitive	-Shape -Counting distribution, no mathematical model
Disadvantages	Not appropriate for very diluted or very concentrated samples	-Retention of particles to the membrane -Retention time independent of the nature of the particles -Low recovery			Possible dissolution due to several dilutions	No size information	-Possible denaturation or aggregation by sample preparation -Not representative of all the sample

D_h: hydrodynamic diameter. RMS: mean square radius. PDI: polydispersity index.
Estimated scores of the methodologies: (+++) extremely high, (++) very high, (+) high, (+/−) moderate and (−) low.

respectively. For the chocolate candies, the mean diameter obtained in those conditions was 135 ± 8 nm and 77 ± 4 nm for undiluted and diluted sample, respectively. Values for these two samples were quite similar to those determined by the other techniques. For the sunscreen, a better accord was obtained when the sample was diluted because of the high concentration of both ionic Ti and TiO_2 NPs in the sample as indicated in the label of the product TiO_2/TiO_2(nano). The sugar-coated candies extracts contained lower levels of Ti as ionic or as NPs, and the diameter obtained without dilution seemed more suitable.

3.2.3. NPs analysis of real samples by SEM and TEM investigations

Results achieved by TEM and SEM are shown in Fig. 5.

For the chocolate candies, TEM images of filtrated extracts (Fig. 5A) showed a reduced number of almost spherical particles with a size in the range 43–49 nm, which were in the form of large aggregates of 160 nm. Non-filtrated chocolate candies extracts were then tested, showing a higher number of particles than in the previous experiment (Fig. 5B and C). In Fig. 5B, primary particles with spherical and oval shapes of approximately 97–100 nm were observed, but aggregated as well as large particles of 200–240 nm were also present. Images of another aliquot (Fig. 5C) showed larger aggregates of 700 nm with primary particles of 80–130 nm, being 90–100 nm the most common size as indicated in the histogram of Fig. 5D. Drops of less dense elements (light grey color) were also observed in Fig. 5C, that could probably be fat co-extracted from chocolate.

SEM images of non-filtrated but centrifuged extract of chocolate candies (Fig. 5E and F) showed large spherical organic particles of 18–30 μm covered by smaller particles (light color) with a spherical or oval shape that can be attributed to TiO_2. The sizes of these particles were in the range of 100–300 nm, being 70–120 nm the most abundant sizes.

TEM image of filtrated extract of the sunscreen sample (Fig. 5G) showed the presence of non-spherical NPs corresponding to several types of inorganic particles as different colors, which are generally attributed to different densities. This concorded with the label of the product, indicating the presence of TiO_2 NPs but also $Al(OH)_3$ and iron (hydr-)oxides. Large aggregates of 300–600 nm were present but small spherical or oval particles with sizes in the range of 60–180 were also observed, being 100–110 nm the most abundant sizes as indicated in the histogram (Fig. 5H).

The size distribution was calculated for the two samples considering results from DLS, AF4-MALS-ICP-MS and spICP-MS to evaluate if the studied samples complied with the regulation. As observed in Fig. S6A (Appendix) for the sunscreen, 50% of the particles had a size lower than 74 nm for DLS and AF4-MALS-ICP-MS and lower than 70 nm for spICP-MS. As a conclusion, for the sunscreen, all the techniques displayed that 50% of the particles had a size lower than 100 nm, thus they can be considered as NMs according to the recommended definition of the EC. For the sugar-coated chocolate candies (Fig. S6B (Appendix)), 50% of the particles had a size lower than 89 nm by DLS, 70 nm by AF4-MALS-ICP-MS and 115 nm by spICP-MS. This sample can be considered as NMs according to AF4-MALS-ICP-MS and DLS techniques, but as non-nano using spICP-MS.

4. Conclusions

Different techniques have been applied in this work to evaluate their potential for the measurement of the size of NPs on a routine basis by analyzing two test samples which supposedly contain NPs. All methodologies applied in this work allow evaluating the presence of NPs and characterizing the size and composition of the particles in the studied samples. The development of these protocols can help to follow with the food and cosmetics labeling regulations towards implementation in the industry and quality control laboratories. Ti-containing NPs were found in the range of 80–110 nm for sunscreen and 100–150 nm for sugar-coated chocolate candies. The diameter obtained by each technique was not really comparable because light scattering techniques provided information about the hydrodynamic diameter (dense core and hydration layer), whereas spICP-MS and TEM measured the particle dense core.

Table 6 shows a comparison of the techniques employed in this work considering several criteria, such as the price, availability, given information, rapidity and sensitivity. In terms of routine analysis, DLS can be selected as the fastest technique for a rapid screening of the presence/absence of NPs. Although DLS is a simple, rapid and cheap technique that could be used for checking the sample preparation procedure, this instrument presents several limitations for polydisperse and/or very diluted samples.

spICP-MS is a good option for routine analysis, probably, the most suitable technique for routine laboratories since it provides good sensitivity and simultaneous information of dissolved ion and NPs (size and composition) of metallic composition by selection of the *m/z* relation and mass fraction.

AF4-MALS provides information about the size distribution or particle size fractionation due to the different retention time of the particles in the AF4 channel. The coupling of AF4-MALS to ICP-MS provides a very visual overview of the composition and the size of the particles present in a sample. However, AF4-MALS-ICP-MS is not completely appropriate for routine evaluations because this technique is still difficult to implement, involving long analysis time and tedious data interpretation. Even if the composition of particles cannot be directly obtained with the microscope used in this work, electron microscopy could be a good confirmation technique if EDXRF can be used to determine the chemical composition and shape of particles.

Acknowledgement

I. de la Calle thanks Xunta de Galicia for financial support as a postdoctoral researcher of the I2C program (POS-A/2013/146 and POS-B/2017/012-PR) and cofinancing by the European Social Funding P.P. 0000 421S 140.08 and UT2A/ADERA for giving her the opportunity to learn and research in their research center and for their help and advice.

Appendix A. Supplementary data

Supplementary data to this article can be found online at https://doi.org/10.1016/j.sab.2018.05.012.

References

[1] European Commission, Commission recommendation of 18 October 2011 on the definition of nanomaterial (text with EEA relevance) (2011/696/EU), Off. J. Eur. Union (2011) 275/38–275/40.
[2] European Commission, Regulation (EC) no 1223/2009 of the European parliament and of the council of 30 November 2009 on cosmetic products, Off. J. Eur. Union (2009) 342/59–342/209.
[3] European Commission, Regulation (EU) no 1169/2011 of the European parliament and of the council of 25 October 2011 on the provision of food information to consumers, amending Regulations (EC) No 1924/2006 and (EC) No 1925/2006 of the European Parliament and of the Council, and repealing Commission Directive 87/250/EEC, Council Directive 90/496/EEC, Commission Directive 1999/10/EC, Directive 2000/13/EC of the European Parliament and of the Council, Commission Directives 2002/67/EC and 2008/5/EC and Commission Regulation (EC) No 608/2004, Off. J. Eur. Union (2011) 304/18–304-63.
[4] Commission Regulation, (EU) 2016/621 of 21 April 2016 Amending Annex VI to Regulation (EC) No 1223/2009 of the European Parliament and of the Council on Cosmetic Products (Text With EEA Relevance), (2016) http://data.europa.eu/eli/reg/2016/621/oj/eng (accessed February 20, 2018).
[5] EFSA Panel on Food Additives and Nutrient Sources added to Food (ANS), Re-evaluation of titanium dioxide (E 171) as a food additive, EFSA J. 14 (2016), http://dx.doi.org/10.2903/j.efsa.2016.4545.
[6] SCSS, Guidance on the safety assessment of nanomaterials in/cosmetics (opinion document) SCSS/1484/12, https://www.google.es/url?sa=t&rct=j&q=&esrc=s&source=web&cd=1&cad=rja&uact=8&ved=0CCQQFjAAahUKEwitt8_63ofHAhWBcz4KHet9A_I&url=http%3A%2F%2Fec.europa.eu%2Fhealth%2Fscientific_committees%2Fconsumer_safety%2Fdocs%2Fsccs_s_005.pdf&ei=Uai8Ve3KF4Hn-QHr-42QDw&usg=AFQjCNHVxGo6TU9BJ7IvhMiMzWeyd2OyZw

&bvm=bv.99261572,d.cWw, (2011).
[7] P.J. Lu, W.L. Cheng, S.C. Huang, Y.P. Chen, H.K. Chou, H.F. Cheng, Characterizing titanium dioxide and zinc oxide nanoparticles in sunscreen spray, Int. J. Cosmet. Sci. 37 (2015) 620–626, http://dx.doi.org/10.1111/ics.12239.
[8] C. Contado, A. Pagnoni, TiO2 in commercial sunscreen lotion: flow field-flow fractionation and ICP-AES together for size analysis, Anal. Chem. 80 (2008) 7594–7608, http://dx.doi.org/10.1021/ac8012626.
[9] I. López-Heras, Y. Madrid, C. Cámara, Prospects and difficulties in TiO_2 nanoparticles analysis in cosmetic and food products using asymmetrical flow field-flow fractionation hyphenated to inductively coupled plasma mass spectrometry, Talanta 124 (2014) 71–78, http://dx.doi.org/10.1016/j.talanta.2014.02.029.
[10] M.K. Butler, T.W. Prow, Y.-N. Guo, L.L. Lin, R.I. Webb, D.J. Martin, High-pressure freezing/freeze substitution and transmission electron microscopy for characterization of metal oxide nanoparticles within sunscreens, Nanomedicine 7 (2012) 541–551, http://dx.doi.org/10.2217/nnm.11.149.
[11] A. Samontha, J. Shiowatana, A. Siripinyanond, Particle size characterization of titanium dioxide in sunscreen products using sedimentation field-flow fractionation-inductively coupled plasma-mass spectrometry, Anal. Bioanal. Chem. 399 (2011) 973–978, http://dx.doi.org/10.1007/s00216-010-4298-z.
[12] Z.A. Lewicka, A.F. Benedetto, D.N. Benoit, W.W. Yu, J.D. Fortner, V.L. Colvin, The structure, composition, and dimensions of TiO2 and ZnO nanomaterials in commercial sunscreens, J. Nanopart. Res. 13 (2011) 3607–3617, http://dx.doi.org/10.1007/s11051-011-0438-4.
[13] C. Botta, J. Labille, M. Auffan, D. Borschneck, H. Miche, M. Cabié, A. Masion, J. Rose, J.-Y. Bottero, TiO2-based nanoparticles released in water from commercialized sunscreens in a life-cycle perspective: structures and quantities, Environ. Pollut. 159 (2011) 1543–1550, http://dx.doi.org/10.1016/j.envpol.2011.03.003.
[14] C. Lorenz, K. Tiede, S. Tear, A. Boxall, N. Von Goetz, K. Hungerbühler, Imaging and characterization of engineered nanoparticles in sunscreens by electron microscopy, under wet and dry conditions, Int. J. Occup. Environ. Health 16 (2010) 406–428, http://dx.doi.org/10.1179/oeh.2010.16.4.406.
[15] K.M. Tyner, A.M. Wokovich, W.H. Doub, L.F. Buhse, L.-P. Sung, S.S. Watson, N. Sadrieh, Comparing methods for detecting and characterizing metal oxide nanoparticles in unmodified commercial sunscreens, Nanomedicine 4 (2009) 145–159, http://dx.doi.org/10.2217/17435889.4.2.145.
[16] J. Labille, J. Feng, C. Botta, D. Borschneck, M. Sammut, M. Cabie, M. Auffan, J. Rose, J.-Y. Bottero, Aging of TiO2 nanocomposites used in sunscreen. Dispersion and fate of the degradation products in aqueous environment, Environ. Pollut. 158 (2010) 3482–3489, http://dx.doi.org/10.1016/j.envpol.2010.02.012.
[17] A. Philippe, G.E. Schaumann, Evaluation of hydrodynamic chromatography coupled with UV-visible, fluorescence and inductively coupled plasma mass spectrometry detectors for sizing and quantifying colloids in environmental media, PLoS ONE 9 (2014) e90559, , http://dx.doi.org/10.1371/journal.pone.0090559.
[18] Y. Dan, H. Shi, X. Liang, S. Stephan, Measurement of Titanium Dioxide Nanoparticles in Sunscreen Using Single Particle ICP-MS, Perkin-Elmer, 2015, http://www.perkinelmer.com/CMSResources/Images/44-171045APP_011990_01-NexION-350D-TiO2-NPs-in-Sunscreen.pdf.
[19] V. Nischwitz, H. Goenaga-Infante, Improved sample preparation and quality control for the characterisation of titanium dioxide nanoparticles in sunscreens using flow field flow fractionation on-line with inductively coupled plasma mass spectrometry, J. Anal. At. Spectrom. 27 (2012) 1084–1092, http://dx.doi.org/10.1039/C2JA10387G.
[20] C. Contado, A. Pagnoni, TiO2 nano- and micro-particles in commercial foundation creams: field flow-fractionation techniques together with ICP-AES and SQW voltammetry for their characterization, Anal. Methods 2 (2010) 1112–1124, http://dx.doi.org/10.1039/C0AY00205D.
[21] R. Peters, G. van Bemmel, Z. Herrera-Rivera, H.P.F.G. Helsper, H.J.P. Marvin, S. Weigel, P.C. Tromp, A.G. Oomen, A.G. Rietveld, H. Bouwmeester, Characterization of titanium dioxide nanoparticles in food products: analytical methods to define nanoparticles, J. Agric. Food Chem. 62 (2014) 6285–6293, http://dx.doi.org/10.1021/jf5011885.
[22] A. Weir, P. Westerhoff, L. Fabricius, K. Hristovski, N. von Goetz, Titanium dioxide nanoparticles in food and personal care products, Environ. Sci. Technol. 46 (2012) 2242–2250, http://dx.doi.org/10.1021/es204168d.
[23] X.-X. Chen, B. Cheng, Y.-X. Yang, A. Cao, J.-H. Liu, L.-J. Du, Y. Liu, Y. Zhao, H. Wang, Characterization and preliminary toxicity assay of nano-titanium dioxide additive in sugar-coated chewing gum, Small Weinh. Bergstr. Ger. 9 (2013) 1765–1774, http://dx.doi.org/10.1002/smll.201201506.
[24] X. Song, R. Li, H. Li, Z. Hu, A. Mustapha, M. Lin, Characterization and quantification of zinc oxide and titanium dioxide nanoparticles in foods, Food Bioprocess Technol. 7 (2014) 456–462, http://dx.doi.org/10.1007/s11947-013-1071-2.
[25] D. Beltrami, D. Calestani, M. Maffini, M. Suman, B. Melegari, A. Zappettini, L. Zanotti, U. Casellato, M. Careri, A. Mangia, Development of a combined SEM and ICP-MS approach for the qualitative and quantitative analyses of metal microparticles and sub-microparticles in food products, Anal. Bioanal. Chem. 401 (2011) 1401–1409, http://dx.doi.org/10.1007/s00216-011-5149-2.
[26] M.E. Hoque, K. Khosravi, K. Newman, C.D. Metcalfe, Detection and characterization of silver nanoparticles in aqueous matrices using asymmetric-flow field flow fractionation with inductively coupled plasma mass spectrometry, J. Chromatogr. A 1233 (2012) 109–115.
[27] M. Baalousha, B. Stolpe, J.R. Lead, Flow field-flow fractionation for the analysis and characterization of natural colloids and manufactured nanoparticles in environmental systems: a critical review, J. Chromatogr. A 1218 (2011) 4078–4103, http://dx.doi.org/10.1016/j.chroma.2011.04.063.
[28] F. Laborda, J. Jiménez-Lamana, E. Bolea, J.R. Castillo, Critical considerations for the determination of nanoparticle number concentrations, size and number size distributions by single particle ICP-MS, J. Anal. At. Spectrom. 28 (2013) 1220–1232, http://dx.doi.org/10.1039/C3JA50100K.
[29] D.M. Mitrano, A. Barber, A. Bednar, P. Westerhoff, C.P. Higgins, J.F. Ranville, Silver nanoparticle characterization using single particle ICP-MS (SP-ICP-MS) and asymmetrical flow field flow fractionation ICP-MS (AF4-ICP-MS), J. Anal. At. Spectrom. 27 (2012) 1131, http://dx.doi.org/10.1039/c2ja30021d.
[30] R. Peters, Z.H. Rivera, G. van Bemmel, H.J.P. Marvin, S. Weigel, H. Bouwmeester, Development and validation of single particle ICP-MS for sizing and quantitative determination of nano-silver in chicken meat, Anal. Bioanal. Chem. 406 (2014) 3875–3885, http://dx.doi.org/10.1007/s00216-013-7571-0.
[31] P. Masson, Quality control techniques for routine analysis with liquid chromatography in laboratories, J. Chromatogr. A 1158 (2007) 168–173, http://dx.doi.org/10.1016/j.chroma.2007.03.003.
[32] C.A. Schneider, W.S. Rasband, K.W. Eliceiri, NIH Image to ImageJ: 25 years of image analysis, Nat. Methods 9 (7) (2012) 671–675.
[33] Y. Yang, K. Doudrick, X. Bi, K. Hristovski, P. Herckes, P. Westerhoff, R. Kaegi, Characterization of food-grade titanium dioxide: the presence of nanosized particles, Environ. Sci. Technol. 48 (2014) 6391–6400, http://dx.doi.org/10.1021/es500436x.
[34] B. Jovanović, V.J. Cvetković, T.L. Mitrović, Effects of human food grade titanium dioxide nanoparticle dietary exposure on *Drosophila melanogaster* survival, fecundity, pupation and expression of antioxidant genes, Chemosphere 144 (2016) 43–49, http://dx.doi.org/10.1016/j.chemosphere.2015.08.054.
[35] B. Jovanović, Critical review of public health regulations of titanium dioxide, a human food additive, Integr. Environ. Assess. Manag. 11 (2015) 10–20, http://dx.doi.org/10.1002/ieam.1571.
[36] A.A. Lizunova, E.G. Kalinina, I.V. Beketov, V.V. Ivanov, Development of reference materials for the diameter of nanoparticles of colloidal solutions of aluminum oxide and titanium dioxide, Meas. Tech. 57 (2014) 848–854, http://dx.doi.org/10.1007/s11018-014-0547-4.
[37] W. Dudefoi, H. Terrisse, M. Richard-Plouet, E. Gautron, F. Popa, B. Humbert, M.-H. Ropers, Criteria to define a more relevant reference sample of titanium dioxide in the context of food: a multiscale approach, Food Addit. Contam. A 34 (2017) 653–665, http://dx.doi.org/10.1080/19440049.2017.1284346.
[38] M. Hassellöv, R. Kaegi, Analysis and characterization of manufactured nanoparticles in aquatic environments, in: J.R. Lead, E. Smith (Eds.), Environ. Hum. Health Impacts Nanotechnol, John Wiley & Sons, 2009, pp. 211–266.
[39] R.B. Reed, C.P. Higgins, P. Westerhoff, S. Tadjiki, J.F. Ranville, Overcoming challenges in analysis of polydisperse metal-containing nanoparticles by single particle inductively coupled plasma mass spectrometry, J. Anal. At. Spectrom. 27 (2012) 1093–1100, http://dx.doi.org/10.1039/C2JA30061C.
[40] H.C. Poynton, J.M. Lazorchak, C.A. Impellitteri, M.E. Smith, K. Rogers, M. Patra, K.A. Hammer, H.J. Allen, C.D. Vulpe, Differential gene expression in *Daphnia magna* suggests distinct modes of action and bioavailability for ZnO nanoparticles and Zn ions, Environ. Sci. Technol. 45 (2011) 762–768, http://dx.doi.org/10.1021/es102501z.
[41] B. Bocca, E. Sabbioni, I. Mičetić, A. Alimonti, F. Petrucci, Size and metal composition characterization of nano- and microparticles in tattoo inks by a combination of analytical techniques, J. Anal. At. Spectrom. 32 (2017) 616–628, http://dx.doi.org/10.1039/C6JA00210B.
[42] H.E. Pace, N.J. Rogers, C. Jarolimek, V.A. Coleman, C.P. Higgins, J.F. Ranville, Determining transport efficiency for the purpose of counting and sizing nanoparticles via single particle inductively coupled plasma mass spectrometry, Anal. Chem. 83 (2011) 9361–9369, http://dx.doi.org/10.1021/ac201952t.
[43] S. Candás-Zapico, D.J. Kutscher, M. Montes-Bayón, J. Bettmer, Single particle analysis of TiO2 in candy products using triple quadrupole ICP-MS, Talanta 180 (2018) 309–315, http://dx.doi.org/10.1016/j.talanta.2017.12.041.
[44] J. Vidmar, R. Milačič, J. Ščančar, Sizing and simultaneous quantification of nanoscale titanium dioxide and a dissolved titanium form by single particle inductively coupled plasma mass spectrometry, Microchem. J. 132 (2017) 391–400, http://dx.doi.org/10.1016/j.microc.2017.02.030.
[45] T. Zheng, S. Bott, Q. Huo, Techniques for accurate sizing of gold nanoparticles using dynamic light scattering with particular application to chemical and biological sensing based on aggregate formation, ACS Appl. Mater. Interfaces 8 (2016) 21585–21594, http://dx.doi.org/10.1021/acsami.6b06903.
[46] P. Krystek, J. Tentschert, Y. Nia, B. Trouiller, L. Noël, M.E. Goetz, A. Papin, A. Luch, T. Guérin, W.H. de Jong, Method development and inter-laboratory comparison about the determination of titanium from titanium dioxide nanoparticles in tissues by inductively coupled plasma mass spectrometry, Anal. Bioanal. Chem. 406 (2014) 3853–3861, http://dx.doi.org/10.1007/s00216-013-7580-z.
[47] N. Bendixen, S. Losert, C. Adlhart, M. Lattuada, A. Ulrich, Membrane–particle interactions in an asymmetric flow field flow fractionation channel studied with titanium dioxide nanoparticles, J. Chromatogr. A 1334 (2014) 92–100, http://dx.doi.org/10.1016/j.chroma.2014.01.066.
[48] B. Fadeel, A.E. Garcia-Bennett, Better safe than sorry: understanding the toxicological properties of inorganic nanoparticles manufactured for biomedical applications, Adv. Drug Deliv. Rev. 62 (2010) 362–374, http://dx.doi.org/10.1016/j.addr.2009.11.008.
[49] C. Larue, H. Castillo-Michel, S. Sobanska, N. Trcera, S. Sorieul, L. Cécillon, L. Ouerdane, S. Legros, G. Sarret, Fate of pristine TiO2 nanoparticles and aged paint-containing TiO2 nanoparticles in lettuce crop after foliar exposure, J. Hazard. Mater. 273 (2014) 17–26, http://dx.doi.org/10.1016/j.jhazmat.2014.03.014.
[50] J. Gigault, V.A. Hackley, Observation of size-independent effects in nanoparticle retention behavior during asymmetric-flow field-flow fractionation, Anal. Bioanal. Chem. 405 (2013) 6251–6258, http://dx.doi.org/10.1007/s00216-013-7055-2.
[51] O. Geiss, C. Cascio, D. Gilliland, F. Franchini, J. Barrero-Moreno, Size and mass

determination of silver nanoparticles in an aqueous matrix using asymmetric flow field flow fractionation coupled to inductively coupled plasma mass spectrometer and ultraviolet–visible detectors, J. Chromatogr. A 1321 (2013) 100–108, http://dx.doi.org/10.1016/j.chroma.2013.10.060.

[52] J. Gigault, T.M. Nguyen, J.M. Pettibone, V.A. Hackley, Accurate determination of the size distribution for polydisperse, cationic metallic nanomaterials by asymmetric-flow field flow fractionation, J. Nanopart. Res. 16 (2014), http://dx.doi.org/10.1007/s11051-014-2735-1.

[53] B. Schmidt, K. Loeschner, N. Hadrup, A. Mortensen, J.J. Sloth, C. Bender Koch, E.H. Larsen, Quantitative characterization of gold nanoparticles by field-flow fractionation coupled online with light scattering detection and inductively coupled plasma mass spectrometry, Anal. Chem. 83 (2011) 2461–2468, http://dx.doi.org/10.1021/ac102545e.

[54] S. Lee, X. Bi, R.B. Reed, J.F. Ranville, P. Herckes, P. Westerhoff, Nanoparticle size detection limits by single particle ICP-MS for 40 elements, Environ. Sci. Technol. 48 (2014) 10291–10300, http://dx.doi.org/10.1021/es502422v.

[55] Y. Dan, W. Zhang, R. Xue, X. Ma, C. Stephan, H. Shi, Characterization of gold nanoparticle uptake by tomato plants using enzymatic extraction followed by single-particle inductively coupled plasma–mass spectrometry analysis, Environ. Sci. Technol. 49 (2015) 3007–3014, http://dx.doi.org/10.1021/es506179e.

[56] C. Degueldre, P.-Y. Favarger, S. Wold, Gold colloid analysis by inductively coupled plasma-mass spectrometry in a single particle mode, Anal. Chim. Acta 555 (2006) 263–268, http://dx.doi.org/10.1016/j.aca.2005.09.021.

[57] Y. Dan, H. Shi, C. Stephan, X. Liang, Rapid analysis of titanium dioxide nanoparticles in sunscreens using single particle inductively coupled plasma–mass spectrometry, Microchem. J. 122 (2015) 119–126, http://dx.doi.org/10.1016/j.microc.2015.04.018.

[58] Standard Reference Material, Titanium Dioxide Nanomaterial, 2012 National Institute of Standards & Technology, 1898.

[59] Y. Zhang, Y. Chen, P. Westerhoff, K. Hristovski, J.C. Crittenden, Stability of commercial metal oxide nanoparticles in water, Water Res. 42 (2008) 2204–2212, http://dx.doi.org/10.1016/j.watres.2007.11.036.

[60] Cordouan Technologies, NanoQ & Vasco Instruction Guide, (2013).

[61] S. Dubascoux, F. Von Der Kammer, I. Le Hécho, M.P. Gautier, G. Lespes, Optimisation of asymmetrical flow field flow fractionation for environmental nanoparticles separation, J. Chromatogr. A 1206 (2008) 160–165, http://dx.doi.org/10.1016/j.chroma.2008.07.032.

[62] J. Soto-Alvaredo, F. Dutschke, J. Bettmer, M. Montes-Bayón, D. Pröfrock, A. Prange, Initial results on the coupling of sedimentation field-flow fractionation (SdFFF) to inductively coupled plasma-tandem mass spectrometry (ICP-MS/MS) for the detection and characterization of TiO_2 nanoparticles, J. Anal. Spectrom. 31 (2016) 1549–1555, http://dx.doi.org/10.1039/C6JA00079G.

[63] J. Virkutyte, S.R. Al-Abed, D.D. Dionysiou, Depletion of the protective aluminum hydroxide coating in TiO2-based sunscreens by swimming pool water ingredients, Chem. Eng. J. 191 (2012) 95–103, http://dx.doi.org/10.1016/j.cej.2012.02.074.

[64] K. Loeschner, J. Navratilova, C. Købler, K. Mølhave, S. Wagner, F. von der Kammer, E.H. Larsen, Detection and characterization of silver nanoparticles in chicken meat by asymmetric flow field flow fractionation with detection by conventional or single particle ICP-MS, Anal. Bioanal. Chem. 405 (2013) 8185–8195, http://dx.doi.org/10.1007/s00216-013-7228-z.